

# Vibrational Dynamics of Carbon Monoxide at the Active Sites of Mutant Heme Proteins<sup>†</sup>

**Jeffrey R. Hill and Dana D. Dlott\***

*School of Chemical Sciences, University of Illinois at Urbana–Champaign, Urbana, Illinois 61801*

**C. W. Rella**

*Hansen Experimental Physics Laboratory, Stanford University, Stanford, California 94305*

**Kristen A. Peterson**

*Department of Chemistry and Biochemistry, New Mexico State University, Las Cruces, New Mexico 88033*

**Sean M. Decatur, Steven G. Boxer, and M. D. Fayer\***

*Department of Chemistry, Stanford University, Stanford, California 94305*

*Received: February 22, 1996; In Final Form: April 2, 1996<sup>®</sup>*

Picosecond mid-IR pump–probe measurements of vibrational relaxation (VR) of CO bound to the active sites of wild-type and mutant myoglobins (Mb) reveal that an approximately linear relationship exists between the protein matrix-induced CO frequency shift and the VR rate. This relation parallels a similar linear relationship seen in a series of heme model compounds where Fe was replaced by Ru and Os. The VR rate of CO in the Mb is sensitive only to the magnitude of protein-induced carbonyl frequency shifts and apparently is not sensitive to the specific details of how the shift is induced, e.g., hydrogen bonding to CO or electrostatic interactions in the heme pocket. CO VR is insensitive to substantial changes in protein structure that do not affect the CO vibrational frequency. These observations suggest that the mechanism of carbon monoxide VR in heme proteins such as Mb occurs by through- $\pi$ -bond anharmonic coupling, which, as shown in prior work, is also the dominant coupling in the model compounds. The experiments indicate that differing protein structures influence VR of CO bound at the active site not by opening and closing channels for vibrational energy flow from CO to the protein but by affecting the rate of energy flow from CO to heme. The rates are determined by the extent of back-bonding, which determines the magnitude of through- $\pi$ -bond anharmonic coupling between CO and heme. The back-bonding and, therefore, the extent of anharmonic coupling are influenced by the electric fields in the heme pocket, which likely differ in the proteins studied here.

## Introduction

In this paper, the relationships between protein structure and protein dynamics at the active site are investigated by using picosecond infrared experiments to probe the vibrational relaxation (VR) of a CO ligand bound at the active site of myoglobin (Mb) mutants. Myoglobin stores dioxygen at an active site located at the central Fe atom of the prosthetic group protoheme (iron(II) protoporphyrin IX).<sup>1</sup> Although bare protoheme alone can bind dioxygen, in biology protein is needed to influence the chemical reactivity of the active site by resisting oxidative degradation and increasing the relative affinity for oxygen versus poisonous carbon monoxide.<sup>1</sup> Many studies have been made of the interactions between the protein and a bound CO ligand at the active site, using techniques including X-ray crystallography,<sup>2–4</sup> <sup>13</sup>C NMR,<sup>5–7</sup> and mid-infrared (mid-IR) spectroscopy.<sup>8–10</sup> Changes in the mid-IR carbonyl stretching spectrum induced by altering the protein structure by genetic engineering have been used to investigate the influence of protein structure on bound ligands at the active site.<sup>8,10,11</sup> Although conventional mid-IR absorption spectroscopy is a powerful technique, it is not capable of revealing the fast vibrational dynamics of ligands bound to the active site.

Recently, mid-IR pump–probe experiments were used to investigate the vibrational relaxation (VR) of vibrationally excited carbon monoxide bound to the active site of Mb<sup>12–14</sup> and heme model compounds.<sup>15</sup> VR is used here to denote the loss of vibrational energy from a vibrationally excited CO to its surroundings.<sup>16</sup> These studies showed that VR of CO bound to heme occurs on the time scale of a few tens of picoseconds<sup>12,13,15</sup> and that VR is little affected by temperature in the 10–300 K range.<sup>14</sup> The lack of temperature dependence indicates the initial VR step does not involve significant coupling to vibrations with frequencies less than 400 cm<sup>-1</sup>.<sup>14,16</sup> The carbonyl VR rate can be influenced by protein structure.<sup>14</sup> For example, two different conformers of Mb-CO were seen in ref 14 to have significantly different VR rates. Studies of carbonyl VR in model heme compounds showed that VR could be influenced by changing the porphyrin structure<sup>14</sup> or by substituting different metal atoms for Fe.<sup>15</sup> The model compound work revealed that VR of carbonyls bound to heme was qualitatively different from VR in previously studied metal carbonyls such as W(CO)<sub>6</sub>.<sup>17</sup> These differences arise because heme is a large aromatic organic molecule with an extensive delocalized  $\pi$ -electron system.

In the present work, we investigate how protein structure influences VR at the active site of Mb by using a series of genetically engineered mutants. Since the cloning and expression of human<sup>18</sup> and sperm whale Mb,<sup>19</sup> the use of mutant Mb proteins has become widespread.<sup>9</sup> Figure 1, taken from a recent

\* Corresponding authors.

<sup>†</sup> This paper is dedicated to Prof. Robin Hochstrasser on the occasion of his 65th birthday.

<sup>®</sup> Abstract published in *Advance ACS Abstracts*, June 15, 1996.

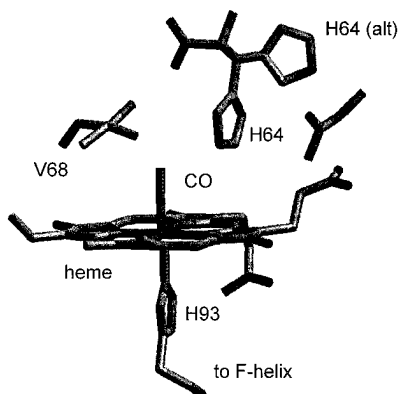


**Figure 1.** Schematic diagram of the active site of wild-type myoglobin (WT Mb), adapted from Yang and Phillips.<sup>3</sup> H64(alt), the alternate position (the up position), is found to dominate at pH 4 and below. The down position for H64 is thought to be representative of the active site structure of the  $A_1$  conformer and the up position representative of the  $A_0$  conformer.

high-resolution X-ray structure of Mb-CO,<sup>3</sup> shows the structure of Mb in the vicinity of the active site. The recombinant proteins used here involve single-point mutations at three of the most important and highly conserved<sup>1</sup> amino acid residues shown in Figure 1: distal histidine H64, valine V68, and proximal histidine H93. Spectroscopic studies of mutant Mb-CO complexes indicate that some mutations strongly influence carbonyl stretching transitions in the mid-IR by affecting the heme-Fe-CO bonding.<sup>8-10</sup> However, the detailed relationships between mid-IR spectra and carbonyl bonding in wild-type (WT) and in mutants have been the subject of lively discussion and debate (reviewed recently in ref 9).

Studies of vibrationally excited CO have been used to investigate dynamics in many condensed-phase systems, including CO dissolved in monatomic and diatomic liquids,<sup>20,21</sup> crystalline CO,<sup>22</sup> organometallic complexes in solution containing CO bound to a single metal atom or a cluster of metal atoms,<sup>17,23-25</sup> CO bound to clean metal surfaces,<sup>26-28</sup> CO bound to heme proteins,<sup>12,13,15,29</sup> and CO bound to model compounds.<sup>15</sup> Although the mechanical dynamics of such complicated systems ordinarily are quite difficult to treat theoretically, CO introduces several useful simplifications. CO is a diatomic molecule that binds to a vast variety of sites, and its electronic structure is well understood.<sup>30</sup> CO vibrational relaxation can be investigated using the techniques of molecular dynamics<sup>31,32</sup> because VR occurs on a suitable (sub-nanosecond) time scale. In contrast to simulations of picosecond time scale photoinduced processes in Mb such as photodissociation<sup>33,34</sup> or vibrational cooling,<sup>35</sup> carbonyl VR occurs solely on the ground electronic potential surface, and simulations need not invoke *ad hoc* assumptions about the nature of heme electronic transitions. The VR of excited CO can also be studied by exact quantum dynamics calculations, which are presently capable of modeling the short-time behavior of a diatomic molecule weakly coupled to harmonic baths of arbitrary complexity. This possibility is especially intriguing in light of recent, highly accurate calculations of the vibrational density of states of a protein.<sup>36</sup>

An initial excitation of CO produced by mid-IR absorption will be localized on CO. Picosecond time scale relaxation of CO vibrational excitation in heme systems occurs via weak anharmonic coupling to other vibrational states of the system,<sup>16</sup> resulting in a transfer of the CO vibrational energy to heme, the heme protein, and the solvent. By using the techniques of synthetic chemistry and site-directed mutagenesis, it is possible to produce a wide variety of tailored Mb structures and analogs. Modified Mb and models, combined with mid-IR dynamics

measurements, for the first time open up the possibility of understanding the details of mechanical energy transfer at the active site of a protein and how protein structure can influence molecular dynamics at the active site.

## Materials and Methods

The preparation and characterization of recombinant mutant human Mb proteins has been discussed previously in ref 18, and the preparation of sperm whale Mb cavity mutants was discussed in ref 37. All Mb samples were dissolved in a mixture of 50:50 glycerol and phosphate buffer at pH = 7. Measurements were made at ambient temperature. In the mid-IR, all the proteins studied exhibit one dominant protein conformer, as indicated by the presence of a single intense carbonyl stretching transition, although a few of the proteins evidenced minor conformers, as discussed in ref 10. The present sensitivity of the pump-probe apparatus permitted measurements only on the dominant conformer of the mutant proteins.

Mid-infrared pump-probe experiments were performed at the Stanford Free Electron Laser Center.<sup>14,17</sup> The pump pulses were 1.5 ps in duration, with an energy of 150 nJ and a spectral FWHM of  $7.3 \text{ cm}^{-1}$ . For each pump pulse, a pair of adjacent 15 nJ probe pulses from the free-electron laser was used. The first pulse of the pair arrives at the unperturbed sample  $\sim 85$  ns before the pump pulse. It is used as an intensity reference for the second pulse. The second pulse, which detects pump-induced absorption changes, reaches the sample within a variable time window of the pump pulse. This window can be varied over a 1 ns range by using a computer-controlled optical delay line. Because of the high  $Q$  of the free-electron laser optical cavity, the two adjacent probe pulses are highly correlated in amplitude. Use of these highly correlated pulses to determine pump-induced absorbance changes makes this method insensitive to laser fluctuations. The probe intensities were measured using a mid-IR detector with a time response faster than the 85 ns interpulse spacing, two gated integrators, and a computer with analog-to-digital converters. The pulses were selected from the free-electron laser high-repetition-rate output using fast acousto-optic modulators<sup>38</sup> and were brought to a common focus of  $100 \mu\text{m}$  diameter on the sample. Experiments were performed with pump and probe polarizations parallel and with the probe pulse at the magic angle. Careful measurements were made to ensure that the vibrational decay constants were not a function of the laser repetition rate or power and that the sample remained chemically stable during data acquisition.

A brief description of the proteins used in this work follows.

**Wild-Type Sperm Whale and Horse Heart Myoglobin (WT SW, WT HH).** The structure in the vicinity of the active site, which is quite similar for both WT proteins, is shown in Figure 1. The mid-IR spectrum of WT provides evidence for at least four conformers, denoted  $A_0$ - $A_3$ , in order of decreasing carbonyl stretching frequency.<sup>39</sup> Under normal conditions in WT,  $A_1$  is the dominant conformer,  $A_0$  is a minor presence, and  $A_2$ - $A_3$  are hardly present.<sup>39</sup> At low pH, the relative population of  $A_0$  increases relative to that of  $A_1$ . It has been suggested by several authors<sup>40</sup> that, among other differences, the  $A_1$  state is characterized by H64 down in the heme pocket and  $A_0$  is characterized by H64 up out of the pocket. A new high-resolution X-ray structure<sup>3</sup> of Mb-CO at normal and low pH shows that H64 can be made to move out of the pocket below pH 4, when the imidazole ring becomes fully protonated. The structures of the active site with H64 down and up [the up state is labeled H64(alt)] are shown in Figure 1. Because the relative population of  $A_0$  increases as pH is decreased,<sup>39,41</sup> these two active site structures are thought to be representative of the  $A_0$  (up) and  $A_1$  (down) conformers.

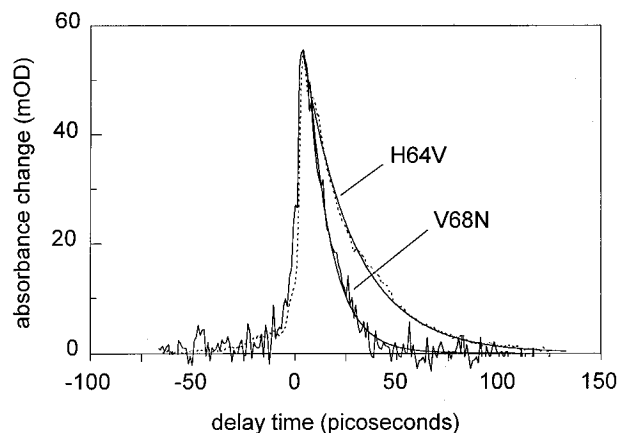


**Figure 2.** Pump-probe decay data obtained with CO bound to human H64V and V68N proteins. The CO stretching frequencies are 1967 and 1917  $\text{cm}^{-1}$ , respectively. The smooth exponential decay curves through the data give vibrational relaxation lifetimes of 21 ( $\pm 2$ ) and 10.5 ( $\pm 2$ ) ps.

**Human H64V.** In H64V, the relatively polar distal histidine residue is replaced by a nonpolar valine. This replacement causes a single sharp band, corresponding to an  $A_0$  conformer, to be observed at 1967  $\text{cm}^{-1}$ , and  $A_1$  is not seen,<sup>11</sup> consistent with the idea that  $A_0$  states involve CO, which is not influenced by a polar H64 residue in the down position.

**Human H64L.** In H64L, the distal histidine is replaced by a nonpolar leucine residue, which is somewhat larger than valine. A single sharp mid-IR band corresponding to an  $A_0$  conformer is observed at 1967  $\text{cm}^{-1}$ , and  $A_1$  is not seen.<sup>11</sup> The H64L mutant has an exceptionally large CO affinity,  $\sim 50$  times greater than WT, which has been attributed to the stabilization of CO by leucine.<sup>9</sup>

**Human V68N.** In V68N, nonpolar V68 is replaced by polar asparagine, resulting in a large carbonyl frequency red shift. Two bands at 1917 and 1933  $\text{cm}^{-1}$  are observed. At 300 K the 1917  $\text{cm}^{-1}$  band (studied here) is dominant.<sup>11</sup> In ref 10, a comparison of the mid-IR and  $^1\text{H}$  NMR spectra of V68N and V68D was used to suggest that replacing V68 with asparagine is accompanied by hydrogen bonding from asparagine to CO.

**Sperm Whale H93G(Im).** In H93G(Im), the proximal histidine is replaced by glycine. Imidazole is added, which becomes bound to Fe in the proximal position, residing in a cavity created by conversion of the histidine to the smaller glycine.<sup>37,42</sup> In H93G(Im), the ligation of Fe is very similar to that of the WT protein, but there is no longer a covalent bond between imidazole and the protein backbone at the F helix (see Figure 1). The sole covalent bond between the heme and the protein in Mb is broken in H93G(Im). Relevant differences between H93G(Im) and WT, e.g., the Fe–N imidazole bond length is 0.3 Å shorter and the imidazole is rotated, have been discussed in detail previously.<sup>42</sup> The mid-IR spectrum is practically identical to the WT spectrum.<sup>37</sup>

## Results

Representative mid-IR picosecond pump-probe data are shown in Figure 2. These decays are due to the recovery of mid-IR absorption saturation induced by pump pulses.<sup>24,25</sup> In all cases, within experimental uncertainty the pump-probe decays were single-exponential functions. Experiments with the probe pulses polarized parallel to the pump and at the magic angle with respect to the pump gave identical results. These experiments eliminate orientational relaxation<sup>17</sup> as a significant contribution to the dynamics of bound CO. The pump-probe decay constant is interpreted to yield the rate of the  $\nu = 1 \rightarrow \nu$

**TABLE 1: Vibrational Lifetimes of CO Bound to Heme Proteins Measured in This Work**

sample	carbonyl stretch frequency ( $\text{cm}^{-1}$ )	carbonyl stretch lifetime (ps)
WT (SW) Mb- $^{13}\text{CO}$ , $A_1$ conformer	1901 ( $\pm 1$ )	17 ( $\pm 2$ )
H93G(Im) (SW), $A_1$ conformer	1946 ( $\pm 1$ )	17 ( $\pm 1$ )
V68N (human), $A_0$ conformer	1917 ( $\pm 1$ )	10.5 ( $\pm 2$ )
H64V (human), <sup>a</sup> $A_0$ conformer	1967 ( $\pm 1$ )	21 ( $\pm 2$ )
H64L (human), $A_0$ conformer	1967 ( $\pm 1$ )	24.5 ( $\pm 1$ )

<sup>a</sup> Some preliminary experiments were run using H64V (SW) protein. These data gave the same CO stretching frequency and essentially the same decay constant as the H64V (human) protein.

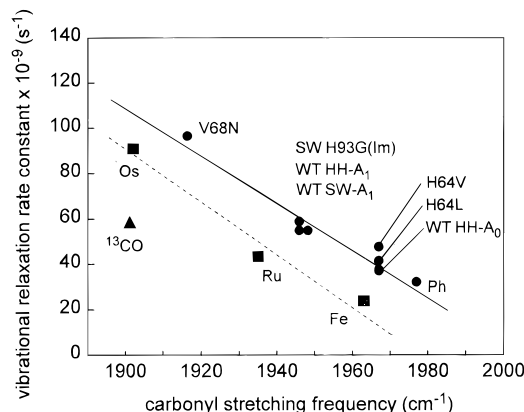


**Figure 3.** Plot of CO vibrational relaxation (VR) rate constants versus CO stretching frequencies. For Mb ( $\bullet$ ), an apparent linear relationship is observed between the frequency and the VR rate constant. Key: SW, sperm whale; WT, wild-type; HH, horse heart; no designation, human; Ph, protoheme. Replacement of  $^{12}\text{CO}$  with  $^{13}\text{CO}$  in WT ( $\blacktriangle$ ,  $^{13}\text{CO}$  denotes  $^{13}\text{CO}$ -WT SW- $A_1$  Mb) induces a significant red shift but no change in the VR rate constant. VR rate constants versus CO frequency for model compounds, M coproporphyrinate I tetraisopropyl ester (CO) (pyridine) in  $\text{CH}_2\text{Cl}_2$  solution (M = Fe, Ru, Os), are denoted by  $\blacksquare$ . The model compound data also show an apparent linear dependence with about the same slope as the Mb data.

= 0 vibrational transition of CO bound to heme.<sup>12–15,24,25</sup> The CO vibrational lifetimes measured in this work are listed in Table 1.

In Figure 3, we plot VR rate constants versus carbonyl stretching frequencies for the proteins listed in Table 1 and for some other proteins studied previously. The latter were WT HH<sup>14</sup> and WT SW.<sup>29</sup> In the WT HH measurements, it was possible to measure the VR rates for the minor  $A_0$  conformer as well as for the major  $A_1$  conformer.<sup>14</sup>

The mid-IR spectra of the distal histidine mutants show only single peaks at essentially the same frequency as the  $A_0$  conformer of WT. Figure 3 shows that these mutants also have the same VR rates as the  $A_0$  conformer of WT. The H93G(Im) mutant has a single peak at essentially the same frequency as the  $A_1$  conformer of WT, and its VR rate is the same as that of  $A_1$  of WT. But in the V68N mutant, the mid-IR absorption peaks are shifted quite a bit from any WT absorptions,<sup>11</sup> and in V68N the VR rate is significantly faster than in WT.

Figure 3 shows that VR rates in Mb vary little across different species. For example, it can be seen in the figure that WT HH- $A_1$  and WT SW- $A_1$  have essentially the same VR lifetime. A preliminary experiment on the SW H64V protein, furnished by Dr. Ellen Chien and Prof. Steven Sligar at the University of Illinois, showed that its VR rate was essentially identical to that of human H64V. Amino acid sequences vary significantly across species. Twenty-seven of the 153 positions are highly conserved across species, including V68, H93, and H64. Nonconserved sites in human, horse, and whale Mb are

populated by a broad variety of different residues. However, these differences have little effect on the overall protein structure, because most substitutions involve residues with similar properties.<sup>1</sup> Our results show that substitutions for even one of the invariant residues can affect VR substantially. Conversely, it is possible for multiple substitutions (in some cases more than 20) in the other sequences to have little effect on VR.

An important result shown in Figure 3 is that, for heme proteins, the VR rates are correlated with the carbonyl stretching frequency. *The rates increase as the carbonyl stretching frequency decreases.* Over the frequency range accessible for this set of proteins, the functional form of VR rate versus frequency is consistent with a linear function, although other relationships that appear to be linear over this frequency range cannot be ruled out. The solid line in Figure 3 is obtained by linear least-squares fitting of the heme protein data. It is interesting, though possibly coincidental, that the VR rate for Fe protoporphyrin IX CO (protoheme-CO, Ph)<sup>29</sup> happens to lie very near this line, even though the protoheme system is quite different from a heme protein. Ph-CO is a bare porphyrin open to the solvent (D<sub>2</sub>O in this case),<sup>13</sup> and the proximal ligand is OH<sup>-</sup> or perhaps D<sub>2</sub>O rather than imidazole. The protoheme data are included in Figure 3 for the sake of comparison, but were not used in fitting the solid line to the protein data.

An experiment was conducted using WT HH <sup>13</sup>CO-Mb. In comparing the A<sub>1</sub> state of <sup>12</sup>CO-Mb to the A<sub>1</sub> state of <sup>13</sup>CO-Mb, we saw a relatively large frequency shift (~40 cm<sup>-1</sup>), but the VR rate was basically unchanged by isotopic substitution.

Figure 3 shows that a quite small absolute change of frequency is associated with a large change in the VR rate. In Figure 3, the absolute fractional change in carbonyl frequency is just a few percent, whereas the VR rates range over a factor of ~3.

In Figure 3, we have also plotted data obtained on model compounds M coproporphyrinate I tetraisopropyl ester (CO) (pyridine) in CH<sub>2</sub>Cl<sub>2</sub> solutions (M = Fe, Ru, Os).<sup>15</sup> For these model compounds, an approximate linear dependence of the VR rate on the carbonyl stretching frequency is also observed. The slope of the dashed line least-squares fit is quite similar to that seen in Mb and its mutants. In fact, given the limited number of points, the slopes could be the same. In unpublished work,<sup>43</sup> we have studied the VR of <sup>13</sup>CO bound to Ru and Os porphyrins. As in Mb, the isotope frequency shift was substantial, but the isotope effect on the VR rate was negligible. Figure 3 also shows that, at a given frequency, the VR rates in the model compounds are about 50% slower than in the heme proteins.

## Discussion

**Brief Summary of Experimental Results.** The most significant results obtained in this study are as follows. Vibrational relaxation of CO bound to mutant Mb occurs on the time scale of tens of picoseconds. Some proteins with different amino acid sequences, and some different conformational states of the same protein, can induce a frequency shift of <sup>12</sup>CO. This induced frequency shift is well correlated with the VR rate; the VR rate increases in an approximately linear fashion as the <sup>12</sup>CO frequency decreases. Isotopic substitution of <sup>13</sup>CO for <sup>12</sup>CO causes a frequency shift by changing the reduced mass, but there is no observable isotope effect on the VR rate. This result allows us to rule out the possibility that the VR rate depends explicitly on the absolute value of the frequency. Therefore, protein-induced effects on the VR rate must be due to a change induced by the protein matrix in the

coupling of the CO vibrational excitation to the rest of the heme protein system. A dependence on the absolute value of the carbonyl frequency might exist, for example, if the density of states for the VR process varied significantly over the ~1900–1980 cm<sup>-1</sup> range of carbonyl stretching frequencies. If a frequency shift simply moved the vibrational frequency to points of higher or lower density of states, thereby causing a change in the VR rate, then the shift caused by the <sup>13</sup>C substitution would also change the VR rate, which does not happen.

Model compounds in CH<sub>2</sub>Cl<sub>2</sub><sup>15</sup> as well as the mutant proteins in glycerol/water evidence an apparent linear relationship between VR rate and frequency, although the absolute value of the VR rate is slightly lower in the heme model compounds. This remarkable observation suggests that the fundamental mechanisms of this effect are the same in both systems and that VR rate does not depend substantially on the specific details of how the shift is induced. In the model compounds, the carbonyl frequency shifts are due to changing the electronic structures of the d<sup>6</sup> metal atoms<sup>15,44</sup> and the associated porphyrin  $\pi$ -electron system to which CO is bound. The changes in electronic structure result in changes in back-bonding from the heme to the CO. In the proteins, frequency shifts are induced by changing the protein matrix. Protein structure modifications can result in strictly electrostatic differences,<sup>10</sup> or they can modify specific interactions such as a hydrogen bond to CO or the number of water molecules in the heme pocket.<sup>9,10</sup> These specific interactions between protein and CO might be expected to give rise to a rather complicated dependence of VR on structure and vibrational frequency. However, such a complicated relationship is not consistent with the simple linear dependence seen in the data, although some specific effects of hydrogen bonding, which could result in small deviations from the observed linear relationship, cannot be ruled out. These results imply that the dominant influence of modifications of the protein on VR is to change the back-bonding from the heme to the CO. This point is discussed further in the following.

**Vibrational Relaxation in Proteins versus Model Compounds.** Figure 3 shows that the absolute values of the frequency-dependent VR rates are about 50% lower in the model compounds than in the mutant proteins. For example, two samples with essentially the same carbonyl frequency, WT HH-A<sub>0</sub> and Fe coproporphyrin, have vibrational lifetimes of 27 and 42 ps, respectively. We have conducted experiments<sup>43</sup> with the intent of better understanding the relationships between these differing molecular structures and the VR rates. In Mb the proximal ligand is imidazole, and in the model compounds it is pyridine. Model compounds that are otherwise similar but are bound to different proximal ligands have been studied. Although some proximal ligands can change the VR rate, substitution of imidazole for pyridine has essentially no effect on VR. The structure of protoheme in Mb differs slightly from that of coproporphyrin, but experiments on compounds with modifications of the porphyrin indicate that the minor differences in structure between protoheme and coproporphyrin are inconsequential (although more substantial structural changes, e.g., sulfonated phenyl groups,<sup>15</sup> can have a consequential effect). The VR rates in the model compounds do depend somewhat on solvent. It takes a rather substantial change in solvent properties to induce a ~50% change in VR rate, e.g., changing CCl<sub>4</sub> to dibutyl phthalate. In the model compounds, coproporphyrin is dissolved in CH<sub>2</sub>Cl<sub>2</sub>. In Mb, heme is embedded in a protein. This is a sufficiently drastic change in solvent (protein environment versus CH<sub>2</sub>Cl<sub>2</sub>) capable of inducing a 50% change in VR rate. Thus, we attribute the differences in absolute VR

rates between the model compounds and the proteins, seen in Figure 3, to differing local solvent environments.

**Pathways for Vibrational Relaxation.** Ultimately the energy deposited by mid-IR excitation of CO becomes randomized throughout the surrounding medium consisting of heme, protein, and solvent.<sup>14</sup> The normal modes of the medium consist of heme vibrations, protein vibrations, and solvent vibrations.<sup>14</sup> Here we use the term vibration to indicate intramolecular normal modes, which principally involve displacements from equilibrium of covalently bonded atoms. In addition, the protein<sup>36</sup> and solvent<sup>45–47</sup> each have a lower frequency continuum of modes, which range from zero frequency to a cutoff lying in the few hundred  $\text{cm}^{-1}$  range. These continua are analogous to the phonon modes<sup>48</sup> of a crystalline solid. The phonon description is precise only for ordered media with well-defined structures, whereas protein and solvent are disordered media with continually evolving structures. The term “instantaneous normal intermolecular modes” is a more precise description of the solvent states.<sup>45–47</sup>

Due to the unusually strong C–O bond in metal carbonyls, there are essentially no fundamental *modes* of the medium resonant with the carbonyl stretch. However, there are a vast number of *states* resonant with this excitation. These states consist of combinations and overtones of the normal modes of the medium. The density of these combination and overtone states increases rapidly with increasing energy. Combinatorial mathematics shows that the density of states increases approximately exponentially with increasing energy.

In the force correlation function description of carbonyl VR,<sup>16</sup> we are not concerned with all of the states of the medium, just states that couple efficiently to the carbonyl stretch. Vibrational energy transfer ordinarily is thought to be more efficient when strong covalent bonds are involved, as opposed to weaker nonbonded interactions.<sup>16</sup> However, there is only a single covalent bond between CO and heme. CO interacts with heme via  $\pi$ -bonded interactions and with protein via a large number of weak nonbonded, and perhaps in some structures hydrogen-bonded, interactions. It is not immediately obvious which of these interactions would be dominant or whether all might compete.

Figure 3 shows that protein clearly influences carbonyl VR. In earlier work,<sup>14</sup> we speculated that protein-induced changes in the VR rate might be due to different protein structures opening or closing channels of vibrational energy transfer for CO  $\rightarrow$  protein. In light of recent experiments on model compounds, an alternative is implied: the role of the protein is not to accept vibrational energy from CO but rather to influence the rate of VR through a primary channel of CO  $\rightarrow$  heme. How that might be accomplished and how it is consistent with the observed dependence of VR rate on carbonyl frequency are discussed in the following.

**Mechanism of Frequency Shifting.** Protein structures that do not affect the carbonyl stretching frequency apparently have no noticeable effect on VR. For example, WT HH-A<sub>1</sub> and WT SW-A<sub>1</sub> have the same carbonyl stretching frequencies and the same VR rates, even though these structures differ at more than 20 amino acid sites.<sup>1</sup> In H93G(Im), the only covalent bond between porphyrin and protein is removed. This structural change does not affect the A<sub>1</sub> frequency, but it might be expected to drastically curtail energy transfer from CO to the proximal side of the protein. However, H93G(Im) has the same VR rate as WT.

Figure 4 is a schematic diagram of the carbonyl binding site, showing some of the  $\sigma$  and  $\pi$  orbitals involved in carbonyl binding to protoheme. The expected geometry of Fe–CO in

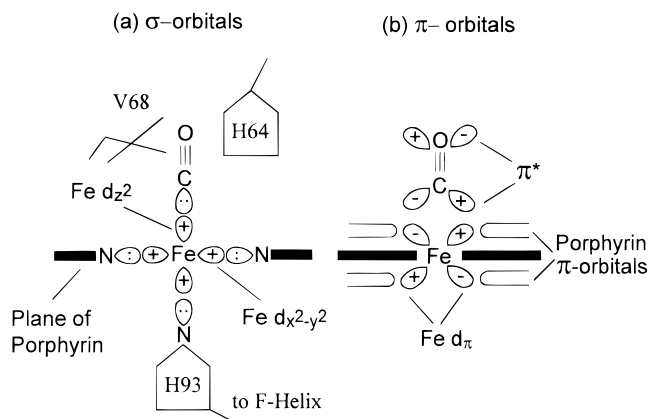


**Figure 4.** Schematic diagram of some of the orbitals involved in CO binding to heme. (a) The through- $\sigma$ -bond anharmonic coupling model for vibrational relaxation involves displacements of CO, which couple directly to motions of Fe. (b) In through- $\pi$ -bond anharmonic coupling, the  $\pi^*$  orbitals of CO interact with the  $\pi$  orbitals of the metalloporphyrin ligand, which produces a coupling between the CO stretch and porphyrin ring vibrations. Different protein structures, e.g., V68 mutants, can shift carbonyl frequency by changing the extent of back-bonding. The rate of vibrational relaxation via through- $\pi$ -bond coupling increases with increasing back-donation from porphyrin to the  $\pi^*$  orbitals of CO.

heme systems is a linear complex oriented perpendicular to the heme plane, based on orbital overlap in the  $\pi$ -back-bonding model of transition metal carbonyl complexes.<sup>9</sup> Infrared dichroism measurements, in principle capable of determining the angle between the CO transition dipole and the heme plane, have been used to suggest the presence of significant protein-induced distortions from perpendicularity in WT Mb.<sup>41</sup> However, many other experiments have suggested that it is difficult for a protein to tilt CO significantly.<sup>49</sup> This view is reinforced by recent infrared dichroism work<sup>50</sup> and polarized infrared measurements of oriented WT Mb single crystals,<sup>51</sup> which presently suggest that the CO transition dipole lies within  $10^\circ$  of perpendicularity.

The predominant factor influencing the stretching frequency of carbonyls bound to  $d^6$  metalloporphyrins is the amount of back-donation (back-bonding) from the combined metal  $d_\pi$  ( $d_{xz}$  and  $d_{yz}$ )/macrocycle  $p_\pi$  orbitals to the carbonyl  $\pi^*$  antibonding orbitals (cf. Figure 4).<sup>44,49</sup> The cause of the change in back-bonding is quite different in the model compounds and mutant proteins. In the model compound series, the polarizability of the  $d^6$  orbitals increases in the order Fe, Ru, Os, and therefore the extent of back-bonding and the carbonyl frequency red shift also increase in this order. In the proteins, the extent of back-bonding between CO and Fe is affected by the protein electric field. Following the usage of ref 10, the term “electrostatic interactions” will be used to denote interactions induced by the electric field of the protein, which change the CO stretching frequency, and the term “specific chemical interactions” will be used to describe variations in bonding, including hydrogen bonds with amino acids in the heme pocket or water in the pocket. An example where electrostatic interactions are important<sup>10</sup> is the case of the V68D mutant, where replacing valine with aspartate does not result in the formation of a hydrogen bond to CO but greatly alters the electrostatic character of the distal pocket. An example where specific chemical interactions are important is the case of the V68N mutant used here, where hydrogen bonding occurs between asparagine and CO, as inferred from <sup>1</sup>H NMR and low-temperature mid-IR measurements.<sup>10</sup> Electrostatic interactions seem to affect back-bonding in an obvious way. Replacement of V68 or H64 with residues with increased positive charge tends to draw electrons from the Fe  $d_\pi$ /macrocycle  $p_\pi$  orbitals into the CO  $\pi^*$  orbitals (see Figure 4), increasing the back-bonding and lowering the carbonyl

stretching frequency. Modified proteins that result in changed specific chemical interactions can also affect back-bonding, and it is not clear that the specific chemical interactions play a role other than the total resultant influence on back-bonding. For example, in V68N, the replacement of nonpolar valine with the polar H-bonding asparagine can increase back-donation to the CO, significantly lowering the carbonyl stretching frequency.<sup>10</sup>

**Mechanism of Vibrational Relaxation in Myoglobin-CO.** Vibrational relaxation occurs through the interaction of the mode initially excited by the laser (called the system; here CO is the system) with other vibrational degrees of freedom of the medium. In theoretical treatments of vibrational relaxation, the interaction of this excitation with the medium is described in terms of the force correlation function.<sup>16,52</sup> The force correlation function has been treated classically<sup>52</sup> and, more recently, quantum mechanically.<sup>16</sup> Initially, it is easier to picture the nature of the process in terms of the classical force correlation function. In addition to the excitation of the system, at finite temperature a vast number of modes of the medium are excited. The excited modes produce a broad spectrum of structural fluctuations. Some or all of the fluctuating modes that are coupled to the system exert forces on it. These forces are described by the force correlation function. The Fourier component of the force correlation function at the vibrational transition frequency of the system drives the relaxation of the system. In the classical description of the force correlation function, only populated modes contribute to the relaxation. The rate of relaxation depends on the occupation numbers,  $n$ , of the modes of the medium that contribute to the Fourier component of the force correlation function at the vibrational transition frequency of the system. The interaction between the excitations of the medium and the system is analogous to stimulated emission by a radiation field of a radiative transition. In the radiation field problem,  $n$  is the number of photons in the field. In the quantum mechanical treatment of the force correlation function, it is found that the probability of relaxation depends on  $(n + 1)$  rather than  $n$ . Therefore, modes that are not thermally populated ( $n = 0$ ) can also contribute to the relaxation process. This is akin to spontaneous emission in a radiative system, where radiative relaxation can occur even in the absence of a radiation field to stimulate emission.

The quantum mechanical treatment of vibrational relaxation is important for understanding the CO relaxation in heme proteins. It has been observed that the vibrational lifetime of CO bound to Mb is essentially temperature independent between room temperature and 10 K.<sup>14</sup> At room temperature,  $kT$  is 200  $\text{cm}^{-1}$ . At room temperature, lower frequency modes below 200  $\text{cm}^{-1}$  will have significant occupation numbers, and much higher frequency modes will have negligible occupation numbers. Therefore, in the 10–300 K range, only the occupation numbers of the lower frequency modes change significantly. If these lower frequency modes were involved in the CO vibrational relaxation, a substantial increase in the vibration lifetime would result from decreasing the temperature from 300 to 10 K. The lack of a temperature dependence demonstrates that only higher frequency modes are involved in the vibrational relaxation. Analysis of temperature-dependent data showed that the higher frequency modes lie in the  $>400 \text{ cm}^{-1}$  range.<sup>15</sup> In a classical treatment, these  $>400 \text{ cm}^{-1}$  modes, which are not thermally populated at the temperatures of interest, could play no role in VR. In the quantum mechanical treatment of VR, the higher frequency modes of the medium coupled to CO play a significant role in VR due to spontaneous emission.

As discussed in ref 15, there are two distinct anharmonic coupling mechanisms for relaxation of the CO vibrational

excitation into heme. These are termed through- $\sigma$ -bond coupling and through- $\pi$ -bond coupling. With reference to Figure 4, the through- $\sigma$ -bond mechanism implies a coupling between the carbonyl stretch and modes that involve displacements of Fe, such as Fe-CO stretching or bending. A quantum mechanical treatment of an analogous scheme, which models the VR of a diatomic AB molecule bound to a third atom M and is coupled to a bath, has been discussed by Benjamin and Reinhardt.<sup>53</sup>

The through- $\pi$ -bond mechanism implies a coupling between the carbonyl stretch and modes of the metalloporphyrin via the  $\pi$  electrons (Fe  $d_{\pi}$ /macrocycle  $p_{\pi}$  orbitals). Structural fluctuations of the macrocycle produce fluctuations of the  $\pi$  electrons, which modulate the back-bonding to the CO. Changes in back-bonding change the vibrational potential. Since force is the derivative of the potential, structural fluctuations of the macrocycle produce fluctuating forces on the CO oscillator. In the context of the classical force correlation function description, the fluctuations are caused by the thermally populated modes of the macrocycle, and the Fourier component at the CO transition frequency drives the relaxation. The quantum mechanical treatment shows that it is not necessary for the modes to be populated because the relaxation of the CO vibration into modes of the macrocycle can occur through spontaneous emission. While not identical to the problem under consideration here, a detailed orbital description of the coupling between a vibrationally excited CO bound to a metallic surface, interacting with labile electrons of the metal, has been presented by Head-Gordon and Tully.<sup>32</sup>

Vibrational relaxation of a relatively small molecule in a solvent, e.g., CO vibrations of  $\text{W}(\text{CO})_6$  in  $\text{CCl}_4$  or  $\text{CHCl}_3$ , involves lower frequency vibrational modes of the molecule, lower frequency vibrational modes of the solvent, and modes of the solvent continuum (instantaneous normal modes).<sup>16,17,23</sup> However carbonyl VR in heme-CO is qualitatively different from the smaller molecule systems because heme is a large molecule; neither a protein nor a solvent is required for VR to occur. The model compound VR data in Figure 4 show that VR in hemes without proteins can be just as efficient as with proteins. It is known from fluorescent emission studies in a supersonic molecular beam of porphyrin in the absence of solvent<sup>54</sup> that the density of vibrational states of free base porphyrin is large enough to permit efficient intramolecular vibrational relaxation processes for an oscillator, provided that the oscillator frequency exceeds  $\sim 900 \text{ cm}^{-1}$ . The heme acts as a bath, providing a sufficiently high density of vibrational states at 2000  $\text{cm}^{-1}$  so that the participation of neither protein nor solvent is required in Mb VR. The through- $\pi$ -bond mechanism qualitatively differs from the through- $\sigma$ -bond mechanism since through- $\pi$ -bond energy transfer from CO need not involve the displacement of Fe, and through- $\pi$ -bond coupling permits mechanical energy to be coupled into the vast number of heme states at the  $\sim 2000 \text{ cm}^{-1}$  energy of the carbonyl oscillator.

In an earlier work, we showed that through- $\pi$ -bond coupling dominated VR of the series of model compounds plotted in Figure 3. In those compounds, the VR rate increased in the order Fe, Ru, Os. This increase is opposite that predicted for through- $\sigma$ -bond coupling.<sup>15</sup> Viewed classically, carbonyl stretch-induced metal atom displacements will be smaller with heavier metal atoms, resulting in slower damping of the CO oscillator. In the language of the force correlation function description, lower frequencies of the modes associated with the heavier metal atoms will result in smaller Fourier coefficients of the force correlation function at the CO transition frequency. Further-

more, the VR rate of through- $\pi$ -bond coupling will increase with increasing electron density in the CO  $\pi^*$  orbital. Since this change in electron density is also responsible for the vibrational frequency shifts, the through- $\pi$ -bond coupling mechanism accounts for the correlation between the frequency shift and the vibrational lifetime. Therefore, the through- $\pi$ -bond coupling mechanism applied to Mb implies that modifications of the protein that induce decreases in the CO stretching frequency will increase the VR rate, consistent with our most significant experimental result.

The evidence that we have accumulated indicates that through- $\pi$ -bond anharmonic coupling dominates vibrational relaxation of CO in Mb, and thus the primary relaxation pathway is from CO directly to heme. An important piece of evidence is the similarity between the frequency dependence of the VR rate in the model compounds and in Mb seen in Figure 3. Other significant observations are the way the VR rate appears to depend only on the protein-induced frequency shift, rather than the details of how this shift is induced, and how the VR rate is insensitive to substantial changes in protein structure that do not affect the carbonyl frequency. Therefore, we conclude that the protein effect on carbonyl VR rate occurs primarily via a mechanism where the protein electric field influences the magnitude of through- $\pi$ -bond coupling for CO  $\rightarrow$  heme, rather than via an active mechanism where different protein structures open up new channels of vibrational energy transfer for CO  $\rightarrow$  protein.

A correlation between the CO frequency shift and the VR rate is useful in understanding the vibrational dynamics at the active site and the influences of structure on the dynamics.<sup>14</sup> Although the change in the absolute value of the CO frequency is small, it is correlated with a large change in the VR rate. Both the frequency and the rate are determined by the vibrational potential.<sup>16</sup> If the potential were perfectly harmonic, there would be no coupling to other modes and nonradiative relaxation of the excited vibration would not occur.<sup>16</sup> It is the anharmonicity of the potential that couples the CO stretch to other modes of the system. The CO transition frequency is the difference between the  $v = 0$  and  $v = 1$  vibrational energies. A change in the nature of the potential may have a small effect on the levels' separation, but a significant effect on the magnitude of the anharmonicity.<sup>16</sup> This is particularly true when the anharmonic coupling is much smaller than the transition frequency, as is the case here. The typical relaxation time for the CO vibration is  $\sim 20$  ps. Viewed classically, for a  $\sim 2000$   $\text{cm}^{-1}$  mode, this implies that the carbonyl oscillator will undergo over 1000 oscillations prior to damping. The VR rate depends on the square of the anharmonic coupling matrix element.<sup>16</sup> Therefore, an increase in the VR rate by a factor of 3 requires an increase in the anharmonic coupling matrix element of only 1.7. This change in the anharmonicity of the potential need not result in a substantial change of the transition frequency.

## Summary

Picosecond mid-IR pump-probe measurements of vibrational relaxation of CO bound to the active site in wild-type and mutant Mb reveal an approximately linear relationship between the protein matrix-induced CO frequency shift and the VR rate. The VR rate is insensitive to substantial changes in protein structure that do not affect the carbonyl stretching frequency. The very simple linear dependence of VR rate on carbonyl frequency indicates that the VR process is not highly dependent on the details of specific protein-CO interactions such as hydrogen bonding. The frequency dependence of the VR rate parallels the dependence observed for a series of model heme compounds,

in which the dominant mechanism for VR is energy transfer CO  $\rightarrow$  heme involving through- $\pi$ -bond anharmonic coupling. These observations lead us to conclude that carbonyl VR in Mb is also dominated by through- $\pi$ -bond coupling between CO and heme. The different structures of the mutant proteins influence the molecular dynamics of bound ligands at the active site, primarily by altering the rate of CO  $\rightarrow$  heme via through- $\pi$ -bond coupling rather than by altering the rate of CO  $\rightarrow$  protein.

**Acknowledgment.** This research was supported by the Medical Free Electron Laser Program, through the Office of Naval Research, Contract NOOO14-91-C-0170 (C.W.R., K.A.P., S.M.D., S.G.B., and M.D.F.). Additional support was provided by the Office of Naval Research, Biology Division, Contract NOOO14-95-1-0259 (D.D.D. and J.R.H.), and by National Science Foundation Grant DMR 94-04806 (D.D.D.). S.G.B. acknowledges support from NIH GM27738. We thank Dr. E. Chien and Prof. S. Sligar for providing the SW H64V mutant used in some initial studies. We thank Prof. Alan Schwettman and Prof. Todd Smith and their research groups for making it possible to perform these experiments at the Stanford Free Electron Laser Center.

## References and Notes

- (1) Antonini, E.; Brunori, M. *Hemoglobin and Myoglobin in Their Reactions with Ligands*; North Holland: Amsterdam, 1971.
- (2) Kuriyan, J.; Wilz, S.; Karplus, M.; Petsko, G. A. *J. Mol. Biol.* **1986**, *192*, 133.
- (3) Yang, F.; Phillips, G. N. *J. Mol. Biol.* **1996**, *256*, 762.
- (4) Quillin, M. L.; Arduini, R. M.; Olson, J. S.; Phillips, G. N., Jr. *J. Mol. Biol.* **1993**, *234*, 140.
- (5) Park, K. D.; Guo, K.; Adebodun, F.; Chiu, M. L.; Sligar, S. G.; Oldfield, E. *Biochemistry* **1991**, *30*, 2333.
- (6) Augspurger, J. D.; Dykstra, C. E.; Oldfield, E. *J. Am. Chem. Soc.* **1991**, *113*, 2447.
- (7) Oldfield, E.; Guo, K.; Augspurger, J. D.; Dykstra, C. E. *J. Am. Chem. Soc.* **1991**, *113*, 7537.
- (8) Braunstein, D. P.; Chu, K.; Egeberg, K. D.; Frauenfelder, H.; Mourant, J. R.; Nienhaus, G. U.; Ormos, P.; Sligar, S. G.; Springer, B. A.; Young, R. D. *Biophys. J.* **1993**, *65*, 2247.
- (9) Springer, B. A.; Sligar, S. G.; Olson, J. S.; Phillips, G. N., Jr. *Chem. Rev.* **1994**, *94*, 699.
- (10) Decatur, S. M.; Boxer, S. G. *Biochem. Biophys. Res. Commun.* **1995**, *212*, 159.
- (11) Balasubramanian, S.; Lambright, D. G.; Boxer, S. G. *Proc. Natl. Acad. Sci. U.S.A.* **1993**, *90*, 4718.
- (12) Hochstrasser, R. M. Femtosecond infrared probing of biomolecules. *Proc. SPIE-Int. Soc. Opt. Eng. (Laser Spectrosc. Biomol.)* **1992**, *1921*, 16.
- (13) Owrutsky, J. C.; Li, M.; Locke, B.; Hochstrasser, R. M. *J. Phys. Chem.* **1995**, *99*, 4842.
- (14) Hill, J. R.; Tokmakoff, A.; Peterson, K. A.; Sauter, B.; Zimdars, D.; Dlott, D. D.; Fayer, M. D. *J. Phys. Chem.* **1994**, *98*, 11213.
- (15) Hill, J. R.; Dlott, D. D.; Fayer, M. D.; Peterson, K. A.; Rella, C. W.; Rosenblatt, M. M.; Suslick, K. S.; Ziegler, C. *Chem. Phys. Lett.* **1995**, *244*, 218.
- (16) Kenkre, V. M.; Tokmakoff, A.; Fayer, M. D. *J. Chem. Phys.* **1994**, *101*, 10618.
- (17) Tokmakoff, A.; Sauter, B.; Fayer, M. D. *J. Chem. Phys.* **1994**, *100*, 9035.
- (18) Varadarajan, R.; Szabo, A.; Boxer, S. G. *Proc. Natl. Acad. Sci. U.S.A.* **1985**, *82*, 5681.
- (19) Springer, B. A.; Sligar, S. G. *Proc. Natl. Acad. Sci. U.S.A.* **1987**, *84*, 8961.
- (20) Anex, D. S.; Ewing, G. E. *J. Phys. Chem.* **1986**, *90*, 1604.
- (21) Disselkamp, R.; Ewing, G. E. *J. Phys. Chem.* **1989**, *93*, 6334.
- (22) Legay-Sommaire, N.; Legay, F. *Chem. Phys.* **1982**, *66*, 315.
- (23) Moore, P.; Tokmakoff, A.; Keyes, T.; Fayer, M. D. *J. Chem. Phys.* **1995**, *103*, 3325.
- (24) Heilweil, E. J.; Cavanagh, R. R.; Stephenson, J. C. *Chem. Phys. Lett.* **1987**, *134*, 181.
- (25) Heilweil, E. J.; Cavanagh, R. R.; Stephenson, J. C. *J. Chem. Phys.* **1988**, *89*, 230.
- (26) Cavanagh, R. R.; Beckerle, J. D.; Casassa, M. P.; Heilweil, E. J.; Stephenson, J. C. *Surface Sci.* **1992**, *269/270*, 113.
- (27) Cavanagh, R. R.; Heilweil, E. J.; Stephenson, J. C. *Surface Sci.* **1993**, *283*, 226.

- (28) Cavanagh, R. R.; Heilweil, E. J.; Stephenson, J. C. *Surface Sci.* **1994**, 299/300, 643.
- (29) Owrutsky, J. C.; Li, M.; Culver, J. P.; Sarisky, M. J.; Yodh, A. G.; Hochstrasser, R. M. Vibrational Dynamics of Condensed Phase Molecules Studied by Ultrafast Infrared Spectroscopy. In *Time Resolved Vibrational Spectroscopy VI*; Lau, A., Ed.; Springer: New York, 1993; Vol. 74; pp 63.
- (30) Walch, S. P.; Goddard, W. A. *J. Am. Chem. Soc.* **1976**, 98, 7908.
- (31) Gomez, M.; Tully, J. C. *J. Vac. Sci. Technol. A* **1993**, 11, 1914.
- (32) Head-Gordon, M.; Tully, J. C. *J. Chem. Phys.* **1992**, 96, 3939.
- (33) Sassaroli, M.; Rousseau, D. L. *J. Biol. Chem.* **1986**, 261, 16292.
- (34) Henry, E. R.; Levitt, M.; Eaton, W. A. *Proc. Natl. Acad. Sci. U.S.A.* **1985**, 82, 2034.
- (35) Henry, E. R.; Eaton, W. A.; Hochstrasser, R. M. *Proc. Natl. Acad. Sci. U.S.A.* **1986**, 83, 8982.
- (36) Roitberg, A.; Gerber, R. B.; Elber, R.; Ratner, M. A. *Science* **1995**, 268, 1319.
- (37) DePillis, G. D.; Decatur, S. M.; Barrick, D.; Boxer, S. G. *J. Am. Chem. Soc.* **1994**, 116, 6981.
- (38) Tokmakoff, A.; Zimdars, D.; Sauter, B.; Francis, R. S.; Kwok, R. S.; Fayer, M. D. *J. Chem. Phys.* **1994**, 101, 1741.
- (39) Ansari, A.; Berendzen, J.; Braunstein, D.; Cowen, B. R.; Frauenfelder, H.; Hong, M. K.; Iben, I. E. T.; Johnson, J. B.; Ormos, P.; Sauke, T. B.; Scholl, R.; Schulte, A.; Steinbach, P. J.; Vittitow, J.; Young, R. D. *Biophys. Chem.* **1987**, 26, 337.
- (40) Ray, G. B.; Li, X.-Y.; Ibers, J. A.; Sessler, J. L.; Spiro, T. G. *J. Am. Chem. Soc.* **1994**, 116, 162.
- (41) Hong, M. K.; Braunstein, D.; Cowen, B. R.; Frauenfelder, H.; Iben, I. E. T.; Mourant, J. R.; Ormos, P.; Scholl, R.; Schulte, A.; Steinbach, P. J.; Xie, A.-H.; Young, R. D. *Biophys. J.* **1990**, 58, 429.
- (42) Barrick, D. *Biochemistry* **1994**, 33, 6546.
- (43) Hill, J. R.; Ziegler, C. J.; Suslick, K. S.; Dlott, D. D.; Rella, C. W.; Fayer, M. D. Submitted for publication in *J. Phys. Chem.*
- (44) Cotton, F. A.; Wilkinson, G. *Advanced Inorganic Chemistry*, 5th ed.; Wiley-Interscience, Inc.: New York, 1988.
- (45) Wu, T. M.; Loring, R. F. *J. Chem. Phys.* **1992**, 97, 8568.
- (46) Xu, B.-C.; Stratt, R. M. *J. Chem. Phys.* **1990**, 92, 1923.
- (47) Seeley, G.; Keyes, T. *J. Chem. Phys.* **1989**, 91, 5581.
- (48) DiBartolo, B. *Optical Interactions in Solids*; John Wiley & Sons, Inc.: New York, 1968.
- (49) Li, X. Y.; Spiro, T. G. *J. Am. Chem. Soc.* **1988**, 110, 6024.
- (50) Lim, M.; Jackson, T. A.; Anfinrud, P. A. *Science* **1995**, 269, 962.
- (51) Hu, S.; Vogel, K. M.; Spiro, T. G. *J. Am. Chem. Soc.* **1994**, 116, 11187.
- (52) Oxtoby, D. W. Vibrational Population Relaxation in Liquids. In *Advances in Chemical Physics*; Wiley-Interscience: New York, 1981; Vol. 47, pp 487.
- (53) Benjamin, I.; Reinhardt, W. P. *J. Chem. Phys.* **1989**, 90, 7535.
- (54) Levy, D. Laser Spectroscopy of Cold Gas-Phase Molecules. In *Annual Reviews in Physical Chemistry*; Rabinovitch, B. S., Ed.; Annual Reviews, Inc.: Palo Alto, CA, 1980; Vol. 31, pp 197.

JP9605414